PAPER

Adaptive Decision Feedback Channel Estimation with Periodic Phase Correction for Frequency-Domain Equalization in DS-CDMA Mobile Radios

Le LIU[†a)], ***Student Member and*** **Fumiyuki ADACHI**[†], ***Member***

SUMMARY Recently, the decision feedback channel estimation based on the minimum mean square error criterion (DF-MMSE-CE) using a fixed DF filter coefficient has been proposed to improve the channel estimation accuracy for DS-CDMA with frequency-domain equalization (FDE). In this paper, we propose adaptive DF (ADF)-MMSE-CE, in which the DF filter coefficient is adapted to changing channel conditions based on a recursive least square (RLS) algorithm. Furthermore, the channel estimate is phase corrected upon the reception of the periodically inserted pilot chip blocks. The average BER performance of DS-CDMA with MMSE-FDE using ADF-MMSE-CE is evaluated by computer simulation in a frequency-selective Rayleigh fading channel and the simulation results show that our proposed scheme is very robust against fast fading.

key words: *DS-CDMA, frequency-domain equalization, adaptive decision feedback, channel estimation*

1. Introduction

In mobile radio communications, the propagation channel consists of a number of resolvable paths having different time delays; each path is a cluster of irresolvable mutlipaths created by reflection and diffraction of the transmitted signal by buildings surrounding a mobile station (MS). The channel transfer function changes rapidly in a random manner in the frequency-domain as well as in the time-domain according to the MSs' movement. Coherent reception needs accurate channel estimation (CE) and so far, many CE schemes have been studied [1]–[15]. A conventional and effective method to accomplish this task is to use periodically inserted pilot symbols, named as pilot-assisted CE. Many improved pilot-assisted CE schemes have been proposed including weighted multi-slot averaging (WMSA) filtering using multiple pilot symbols [2], [3] (the uniform averaging filter [4] is just a special case with equal weighted parameters), polynominal interpolation filtering [5], and least-mean-square (LMS) filtering [6] to reduce the number of pilot symbols and achieve fast convergence. In general, all of them can be regarded as finite impulse response (FIR) filters with different sets of filter coefficients [7]. However, as the fading becomes faster, the tracking ability tends to be lost [3].

The simplest way to improve the tracking ability against fast fading is to increase the pilot insertion rate, but at the price of transmission efficiency. In order to achieve robust channel estimation against fast fading, a pilot-assisted CE using a Wiener filter [8] is optimal, but it requires the knowledge of the unknown channel statistics [9] (e.g., the frequency offset due to the Doppler spread and the average received signal-to-noise power ratio (SNR)). Thus, some adaptive techniques have to be adopted. In [10], a simple adaptive WMSA CE was proposed, taking into account the tradeoff relationship between the noise reduction and the fading tracking ability. However, the performance of adaptive FIR filter depends on the filter order, which needs to be adjusted according to the estimated maximum Doppler frequency.

Recently, the frequency-domain pilot-assisted CE based on the minimum mean square error (MMSE) criterion was proposed for DS-CMDA with frequency-domain equalization (FDE) [11], which incorporates decision feedback (DF) using an infinite impulse response (IIR) filter into MMSE-CE. This improves the fading tracking ability while reducing the loss in the transmission efficiency due to the pilot insertion. The IIR filter coefficient is an important design parameter and the computer simulation results of [11] show that the optimum filter coefficient depends on the signal-to-noise power ratio (SNR) and the Doppler spread. However, the SNR and the Doppler spread vary according to changes in MSs' locations and traveling speeds, respectively. As a result, the fixed IIR filter used in [11] cannot achieve the optimal performance in all cases.

The IIR filter is very effective and desirable since there is only one filter coefficient. In [12], the IIR filter coefficient is adjusted according to the recursive least-square (RLS) algorithm assuming narrowband differential-detected DS-CDMA [12]. We apply this adaptive IIR filter on each frequency component of MMSE-CE. However, due to the relatively low SNR, it is not reliable using a different filter coefficient on each frequency component. Since the channel is almost constant over one block even for large Doppler spread (e.g., the maximum Doppler spread f_D is equal to 2 kHz when an MS's vehicle speed is about 432 km/h at 5 GHz carrier frequency), the fading statistics are identical at all frequencies. In this paper, we propose an adaptive DF (ADF)-MMSE-CE that uses the same filter coefficient for all frequencies and updates the filter coefficient block by block.

Two types of adaptive filters, an IIR filter and a forward linear prediction (FLP) filter, are considered to track

Manuscript received August 4, 2006.
Manuscript revised November 29, 2006.
[†]The authors are with the Dept. of Electrical and Communication Engineering, Tohoku University, Sendai-shi, 980-8585 Japan.
a) E-mail: liule@mobile.ecei.tohoku.ac.jp
DOI: 10.1093/ietcom/e90–b.8.1997

the changing channel conditions and their filter coefficients are updated according to the RLS algorithm. We also give a theoretical analysis for the convergence performance of the ADF filter coefficient. The impact of channel estimation errors on the average BER performance of DS-CDMA with MMSE-FDE is evaluated by computer simulation in a frequency-selective Rayleigh fading channel.

The remainder of this paper is organized as follows. Section 2 presents the transmission system model for DS-CDMA with MMSE-FDE. Section 3 describes the proposed ADF-MMSE-CE. Also presented is the theoretical analysis of the convergence performance of the ADF filter coefficient. Section 4 shows the simulation results for the average BER performance. Finally, we draw the conclusion in Sect. 5.

2. Transmission System Model

2.1 Transmitted Signal

The DS-CDMA transmission system model is illustrated in Fig. 1. At a transmitter, a binary data sequence is transformed into a data-modulated symbol sequence. Then, the nth data symbol $d(n)$ is spread by the spreading sequence $c(t)$ to obtain the chip sequence $s(t)$, given by

$$s(t) = d(\lfloor t/SF \rfloor)c(t), \tag{1}$$

where SF is the spreading factor, $\lfloor x \rfloor$ is the largest integer smaller than or equal to x and we assume $|d(n)| = |c(t)| = 1$. Then, the resultant chip sequence $s(t)$ is divided into a sequence of N_c-chip blocks. As shown in Fig. 1(b), a known pilot chip block of N_c chips is inserted every $(D-1)$ data chip blocks; one pilot chip block and succeeding $(D-1)$ data chip blocks make a frame. The mth block chip sequence in

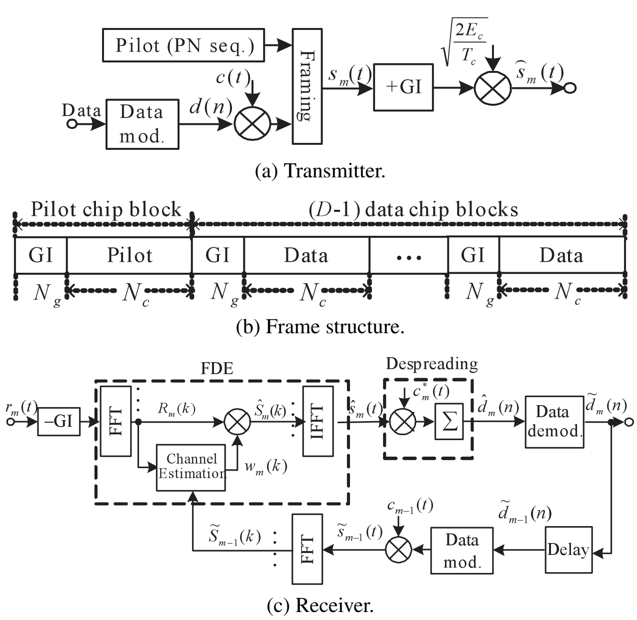

(a) Transmitter.

(b) Frame structure.

(c) Receiver.

Fig. 1 DS-CDMA transmitter/receiver and frame structure.

one frame is denoted by $s_m(t)$, $t = 0 \sim N_c - 1$. Correspondingly, the data in the mth block is denoted by $d_m(n)$, $n = 0 \sim N_c/SF - 1$, the spreading code used in the mth block is denoted by $c_m(t)$, $t = 0 \sim N_c - 1$. The m=iDth chip block corresponds to the pilot chip block in the ith frame. The last N_g chips of each block are copied as a cyclic prefix and inserted into the guard interval (GI) at the beginning of each block. The GI-inserted chip sequence in the mth chip block can be expressed as

$$\hat{s}_m(t) = \sqrt{2E_c/T_c}\, s_m(t \bmod N_c) \tag{2}$$

for $t = -N_g \sim N_c - 1$, where E_c is the average chip energy and T_c is the chip duration.

2.2 Received Signal

The mth block received signal is sampled at the chip rate to obtain

$$r_m(t) = \sum_{l=0}^{L-1} h_{m,l}\hat{s}_m(t - \tau_l) + \eta_m(t), \tag{3}$$

where $h_{m,l}$ and τ_l are respectively the lth path channel gain and the lth path T_c-spaced time delay with $\sum_{l=0}^{L-1} E[|h_{m,l}|^2] = 1$ ($E[\cdot]$ is the ensemble average operation), and $\eta_m(t)$ is the additive white Gaussian noise (AWGN) process with zero-mean and the variance of $2N_0/T_c$ with N_0 being the single-sided power spectrum density. We assume a block-fading channel so that the path gains $\{h_{m,l};\ l = 0 \sim L-1\}$ remain constant over one block interval, but vary block-by-block according to the MSs' movement. Also assumed is that the maximum time delay of the channel is shorter than GI and the maximum Doppler frequency is f_D. In this paper, we consider the normalized Doppler frequency, f_DT, is smaller than 0.02. f_DT=0.02 corresponds to a moving speed of 1500 km/h for a chip rate of 100 Mcps and 5 GHz carrier frequency. If f_DT increases beyond 0.02, the assumption of block fading cannot hold since the channel does not stay constant over one block interval anymore and FDE cannot be properly carried out as discussed in [19].

As shown in the Fig. 1(c), after the removal of GI, $\{r_m(t);\ t = 0 \sim N_c - 1\}$ are decomposed into N_c frequency components $\{R_m(k);\ k = 0 \sim N_c - 1\}$ by using N_c-point fast Fourier transform (FFT). $R_m(k)$ can be expressed as

$$R_m(k) = \sqrt{2E_c/T_c}\, S_m(k)H_m(k) + \Pi_m(k), \tag{4}$$

where $S_m(k)$ is the kth frequency component of the data chip sequence with $E[|S_m(k)|^2]$=1, $H_m(k)$ is the channel gain component with $E[|H_m(k)|^2]$=1, and $\Pi_m(k)$ is the noise component due to the AWGN with zero-mean and the variance of $E[|\Pi_m(k)|^2] = 2N_0/T_c$. They are given by

$$\begin{cases} S_m(k) = \left(1/\sqrt{N_c}\right)\sum_{t=0}^{N_c-1} s_m(t)\exp(-j2\pi kt/N_c) \\ H_m(k) = \sum_{l=0}^{L-1} h_{m,l}\exp(-j2\pi k\tau_l/N_c) \\ \Pi_m(k) = \left(1/\sqrt{N_c}\right)\sum_{t=0}^{N_c-1} \eta_m(t)\exp(-j2\pi kt/N_c) \end{cases}. \quad (5)$$

One-tap FDE is performed on each frequency component as

$$\hat{S}_m(k) = w_m(k)R_m(k), \quad (6)$$

where $w_m(k)$ is the MMSE-FDE weight, given by [13]

$$w_m(k) = \frac{\sqrt{2E_c/T_c}H_m^*(k)}{\left|\sqrt{2E_c/T_c}H_m(k)\right|^2 + 2N_0/T_c}. \quad (7)$$

However, $\sqrt{2E_c/T_c}H_m(k)$ is unknown to the receiver and needs to be estimated. The detailed operation of MMSE-CE is described in Sect. 2.3. After MMSE-FDE, N_c-point inverse FFT (IFFT) is applied to obtain the time-domain chip sequence:

$$\hat{s}_m(t) = \left(1/\sqrt{N_c}\right)\sum_{k=0}^{N_c-1} \hat{S}_m(k)\exp(j2\pi tk/N_c). \quad (8)$$

After despreading, we get the decision variable $\hat{d}_m(n)$ as

$$\hat{d}_m(n) = \frac{1}{SF}\sum_{t=nSF}^{(n+1)SF-1} \hat{s}_m(t)c_m^*(t), \quad (9)$$

based on which the data demodulation for $d_m(n)$ is performed to obtain $\tilde{d}_m(n)$.

2.3 MMSE-CE

Accurate estimation of the channel gain $H_m(k)$ is essential to compute the MMSE-FDE weight in Eq. (7). Since the frequency spectrum of the pilot chip sequence is not necessarily constant over the spreading bandwidth, we consider DF-MMSE-CE [11] in this paper. First, using the kth frequency component of the ith pilot chip block at $m=iD$, $i = 0, 1\ldots,$ MMSE-CE can be applied to obtain the instantaneous channel estimate at $m=iD$. The delay time-domain windowing [14], [15] is performed to get the noise-reduced channel estimate $\bar{H}^P_{m=iD}(k)$, which is used for the detection of $(D-1)$ succeeding data chip blocks ($m = iD+1 \sim (i+1)D-1$). Next, the $(m-1)$th block decision $\tilde{d}_{m-1}(n)$ is fedback as a new pilot for MMSE-FDE of the mth block signal. The current block decision is fedback as a new pilot for MMSE-FDE of the next block signal. Therefore, the $(m-1)$th block decision $\tilde{d}_{m-1}(n)$ is fedback as a reference to detect $\tilde{d}_m(n)$ and one-block delay is always incurred. As shown in Fig. 1(c), $\tilde{d}_{m-1}(n)$ is first re-spread by using $c_{m-1}(t)$ to obtain $\tilde{s}_{m-1}(t)$ and next, an N_c-point FFT is applied to $\{\tilde{s}_{m-1}(t);\ t = 0 \sim N_c-1\}$ to get N_c frequency components $\{\tilde{S}_{m-1}(k);\ k = 0 \sim N_c-1\}$ with $E[|\tilde{S}_{m-1}(k)|^2] = 1$. Then we use this decision feedback to carry out MMSE-CE and the delay time-domain windowing to get the noise-reduced channel estimate $\tilde{H}_{m-1}(k)$.

2.4 CE Filtering

(1) IIR DF Filter
We use a first-order IIR filter [12], [16] to improve the channel estimate, expressed as

$$\bar{H}^{IIR}_m(k) = \alpha\bar{H}^{IIR}_{m-1}(k) + (1-\alpha)\tilde{H}_{m-1}(k) \quad (10)$$

with $m \geq 1$, where α is the IIR filter coefficient. The initial condition is set as $\bar{H}^{IIR}_0(k) = \tilde{H}_0(k) = \bar{H}^P_0(k)$. The MMSE-FDE weight $w_m(k)$ is computed using $\bar{H}^{IIR}_m(k)$ instead of $\sqrt{2E_c/T_c}H_m(k)$ in Eq. (7) to perform MMSE-FDE of the mth block signal. α is an important design parameter to tradeoff between the noise reduction and the tracking ability against fading. In a fast fading channel, α should be smaller to achieve better tracking ability. As the value of α increases, the IIR filter can effectively reduce the noise, but the tracking ability against fading tends to be lost. Therefore, there exists an optimum value in α, which depends on the received SNR and the Doppler spread [11].
(2) FLP DF Filter
Another method to improve the channel estimation accuracy, especially for fast fading, is the FLP filter [12], [16]. We introduce the predictor coefficient μ ($|\mu| \leq 1$) and predict the mth block channel gain as

$$\bar{H}^{FLP}_m(k) = \tilde{H}_{m-1}(k) + \mu(\tilde{H}_{m-1}(k) - \tilde{H}_{m-2}(k)). \quad (11)$$

The MMSE-FDE weight $w_m(k)$ is computed by using $\bar{H}^{FLP}_m(k)$ instead of $\sqrt{2E_c/T_c}H_m(k)$ in Eq. (7). Compared with the IIR filter in Eq. (10), the FLP filter is much simpler, whose output is just decided by two past channel estimates, $\tilde{H}_{m-1}(k)$ and $\tilde{H}_{m-2}(k)$.

The filter coefficients, α and μ, should be adapted to changing channel conditions. The adaptation algorithms for α and μ are described in Sect. 3.1.

3. Adaptive Decision Feedback Filter

The fading channel conditions may vary from time to time with the MSs' movement. In this paper, we apply the RLS adaptive algorithm [16], [17] so that α for the IIR filter and μ for the FLP filter are adjusted according to changing channel conditions.

3.1 Adaptation Algorithm

(1) Adaptive IIR Filter
Equation (10) can be regarded as the single-tap least mean square (LMS) algorithm [16] with the step-size parameter α. In the LMS algorithm, α is defined over the positive range of [0, 1], but here we allow its value to be negative to track statistical variations of the channel gains. We first get the adaptive $\alpha_m(k)$ for each frequency (α in Eq. (10) is denoted

by $\alpha_m(k)$). $\alpha_m(k)$ is updated by using recursive adaptation algorithm as [12]

$$\alpha_m(k) = -\frac{\Theta_m(k)}{\Omega_m(k)} \tag{12}$$

for $k = 0 \sim N_c - 1$, where

$$\begin{cases} \Theta_m(k) = \beta\Theta_{m-1}(k) + \mathrm{Re}\left\{A_m(k)B_m^*(k)\right\} \\ \Omega_m(k) = \beta\Omega_{m-1}(k) + |B_m(k)|^2 \end{cases} \tag{13}$$

and

$$\begin{cases} A_{m-l}(k) = R_{m-l}(k) - \tilde{H}_{m-1-l}(k)\tilde{S}_{m-l}(k) \\ B_{m-l}(k) = \tilde{S}_{m-l}(k)\left\{\tilde{H}_{m-1-l}(k) - \bar{H}^{IIR}_{m-1-l}(k)\right\} \end{cases}. \tag{14}$$

The initial condition is set as $\Theta_0 = 0$ and $\Omega_0 = \delta$ (small positive value).

However, $\alpha_m(k)$ is perturbed by the noise and not reliable. Remember that the fading statistics are identical for all frequencies, $k = 0 \sim N_c - 1$. Instead of using $\alpha_m(k)$ for the kth frequency component, we propose to use a filter coefficient α_m averaged over all the frequencies as

$$\alpha_m = \frac{1}{N_c}\sum_{k=0}^{N_c-1}\alpha_m(k). \tag{15}$$

(2) Adaptive FLP Filter
Similar with adaptive IIR filter, we derive μ_m for adaptive FLP filter, given as

$$\mu_m = \frac{1}{N_c}\sum_{k=0}^{N_c-1}\mu_m(k) \tag{16}$$

with

$$\mu_m(k) = \frac{\Theta'_m(k)}{\Omega'_m(k)}, \tag{17}$$

where

$$\begin{cases} \Theta'_m(k) = \beta\Theta'_{m-1}(k) + \mathrm{Re}\left\{A_m(k)B'^*_m(k)\right\} \\ \Omega'_m(k) = \beta\Omega'_{m-1}(k) + \left|B'_m(k)\right|^2 \end{cases} \tag{18}$$

and

$$\begin{cases} A_{m-l}(k) = R_{m-l}(k) - \tilde{H}_{m-1-l}(k)\tilde{S}_{m-l}(k) \\ B'_{m-l}(k) = \tilde{S}_{m-l}(k)\left\{\tilde{H}_{m-1-l}(k) - \tilde{H}_{m-2-l}(k)\right\} \end{cases}. \tag{19}$$

The initial condition is set as Θ'_0=0 and Ω'_0=δ (small positive value).

Upon the reception of pilot chip block at $m = iD$, $i = 0, 1\ldots$, the IIR filter output $\bar{H}^{IIR}_m(k)$ and the FLP filter output $\bar{H}^{FLP}_m(k)$ are phase rotated as $\left|\bar{H}^{IIR}_m(k)\right|\left(\bar{H}^P_m(k)/\left|\bar{H}^P_m(k)\right|\right)$ and $\left|\bar{H}^{FLR}_m(k)\right|\left(\bar{H}^P_m(k)/\left|\bar{H}^P_m(k)\right|\right)$, respectively, where $\bar{H}^P_{m=iD}(k)$ is the pilot-assisted channel estimate of the ith frame. As a result, the resultant channel estimate becomes in-phase with $\bar{H}^P_{m=iD}(k)$.

3.2 Convergence Analysis

In order to better understand our proposed scheme, we present an approximate analysis on the convergence performances of the IIR filter coefficient α_m and the FLP filter coefficient μ_m in a frequency-selective Rayleigh channel. It is shown in Appendix that α_m converges to

$$\alpha_\infty = 1 + \frac{0.5[\rho(2) - 1]}{1 - \rho(1) + 0.5\,(E_c/N_0)^{-1}\left(N_g/N_c\right)} \tag{20}$$

and μ_m converges to

$$\mu_\infty = -0.5 - \frac{0.5[\rho(2) - \rho(1)]}{1 - \rho(1) + (E_c/N_0)^{-1}\left(N_g/N_c\right)}, \tag{21}$$

where $\rho(n)$ is the time autocorrelation function of path gains $\{h_{m,l};\ l = 0 \sim L-1\}$ and equal to the time autocorrelation of the kth frequency channel gain $H_m(k)$, defined as $E[H_m(k)H^*_{m-n}(k)]$ (as shown in Appendix, $\rho(n)$ is independent of the frequency index k) [18]. Equations (20) and (21) show that α_∞ and μ_∞ are determined considering the tradeoff relationship between the noise reduction and the tracking ability. Assuming the Jakes' model, we have $\rho(n) = J_0(2\pi n f_D T)$, where $J_0(\cdot)$ is the zero-order Bessel function of the first kind. For small $f_D T$ values, $\rho(n)$ can be approximated as $\rho(n) \approx 1 - (\pi n f_D T)^2$. Then, for the IIR filter we have,

$$\alpha_\infty \approx 1 - \frac{2(\pi f_D T)^2}{(\pi f_D T)^2 + 0.5\,(E_c/N_0)^{-1}\left(N_g/N_c\right)}. \tag{22}$$

and for FLP filter, we have

$$\mu_\infty \approx -0.5 + \frac{1.5(\pi f_D T)^2}{(\pi f_D T)^2 + (E_c/N_0)^{-1}\left(N_g/N_c\right)}. \tag{23}$$

When $f_D T \to 0$, we have $\alpha_\infty \approx 1$ for the IIR filter and $\mu_\infty \approx -0.5$ for the FLP filter.

The convergence time and accuracy are dependent on β. The use of smaller β has better tracking ability but less accuracy. The larger β needs longer time for α_m and μ_m to converge. The inverse of $1-\beta$ is roughly a measure of the memory size of the RLS algorithm [17]. For example, when β=0.95, it takes about 20 blocks (one block is about 2.88 μs for a chip rate of 100 Mcps). Since the channel fading statistics change much more slowly compared with the RLS updating process, even β=0.95 can be used in practice.

4. Computer Simulation

Table 1 shows the simulation conditions. We assume ideal sampling timing at the receiver and the channel is an L=16-path frequency-selective Rayleigh block-fading channel having uniform power delay profile (i.e., E[$|h_{m,l}|^2$]=1/L for all m and l).

Table 1 Simulation conditions.

Data modulation	QPSK
Spreading code	OVSF code, SF=16, 64
Block Length	N_c=256
Guard interval	N_g=32
Frame structure	1-pilot+(D–1)-data blocks
Rayleigh channel	L=16, uniform delay profile

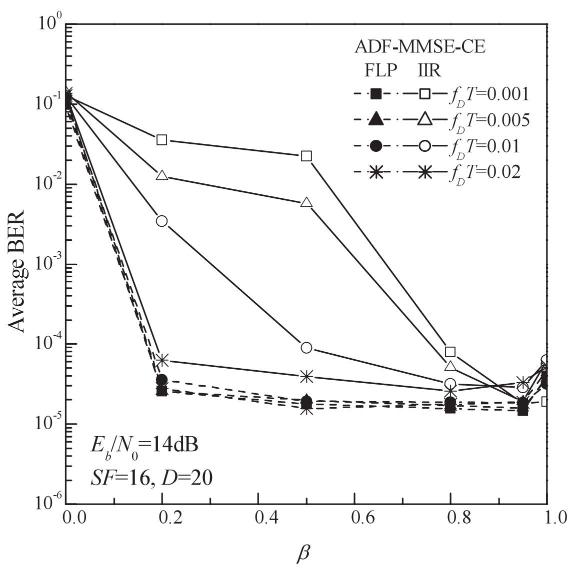

Fig. 2 Impact of forgetting factor β.

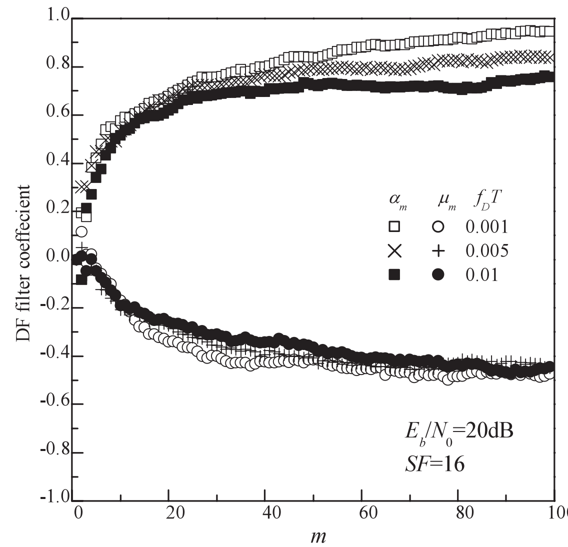

Fig. 3 Convergence rate.

4.1 Impact of Forgetting Factor β

Figure 2 shows the impact of forgetting factor β on the BER performance assuming the average received bit energy-to-AWGN power spectrum density ratio E_b/N_0=14 dB, the spreading factor SF=16, and the normalized Doppler frequency f_DT=0.001 ~ 0.02. E_b/N_0 is defined as $E_b/N_0 = 0.5SF(1 + N_g/N_c)(E_c/N_0)(1 + D^{-1})$ and f_DT=0.001 (0.02) corresponds to a moving speed of 75 km/h (1500 km/h) for a chip rate of 100 Mcps and 5 GHz carrier frequency. The initial value of α_m is set as α_0=0.

We can see that the BER of FLP filter is almost insensitive of β. The reason for this is as follows. Even if f_DT is as high as f_DT=0.02, the channel estimates, $\tilde{H}_{m-1-l}(k)$ and $\tilde{H}_{m-2-l}(k)$, are almost the same, resulting in a very small value of $B'_m(k)$ in Eq. (19). From Eqs. (17) and (18), the FLP filter coefficient $\mu_m(k)$ is approximately given by $\mu_m(k) = \Theta'_m(k)/\Omega'_m(k) \approx \Theta'_{m-1}(k)/\Omega'_{m-1}(k)$ since $B'_m(k) \approx 0$. Therefore, $\mu_m(k)$ is almost the same as $\mu_{m-1}(k)$ irrespective of β. On the other hand, β has great influence on the BER performance of adaptive IIR filter for different f_DT. The use of smaller β has better tracking ability, but α_m varies widely and is not stable enough to get good BER performance. We see that the use of β=0.95 for adaptive IIR filter is suitable for f_DT=0.001 ~ 0.02. If f_DT is less than 0.02, the BER performance doesn't degrade at all. However, if f_DT increases beyond 0.02, the assumption of block fading cannot hold since the channel does not stay constant over one block anymore and FDE cannot be properly carried out as discussed in [19]. As a consequence, the BER performance degrades as f_DT increases beyond 0.02. In the following simulation, we set β to be 0.95 for both adaptive IIR and FLP filter.

Figure 3 shows the convergence rate of α_m for adaptive IIR filter and μ_m for adaptive FIR filter when β=0.95 is used for different f_DT. Although α_0 is set to α_0=0, the value of α_m becomes negative for small m to adaptively track channel variations. We have found by theoretical analysis in Sect. 3.2 that, for slow fading, α_m converges close to 1.0 as time m elapses. The coefficient α_m converges a different value for a different value of f_DT; while the coefficient μ_m converges almost the same value of −0.5 irrespective of f_DT. The reason for this is as follows. α_∞ becomes smaller to improve the tracking ability as f_DT increases. This can be understood from Eq. (22). On the other hand, even if f_DT is as high as f_DT=0.02, the channel estimates, $\tilde{H}_{m-1-l}(k)$ and $\tilde{H}_{m-2-l}(k)$, are almost the same, resulting in a very small value of $B'_m(k)$ in Eq. (19). Since $\rho(2)$ is almost same as $\rho(1)$ and from Eq. (21) we have μ_∞ is always equal to −0.5.

Figure 4 plots the impact of Doppler spread on the DF filter coefficient after convergence when E_b/N_0=20 dB and SF=16. Our performance analysis is an approximate analysis based on the assumption of no decision feedback error and no noise contribution in the IIR filter output. A good agreement can be seen between the theoretical result and the simulation one with μ_∞ when f_DT is smaller than 0.001 and E_b/N_0=20 dB. If f_DT is very small, $\tilde{H}_{m-1-l}(k) \approx \tilde{H}_{m-2-l}(k)$ and hence $B'_{m-l}(k) \approx 0$. As a consequence, the decision feedback error does not influence the value of μ_∞. However, the decision feedback error impacts the value of α_∞. As f_DT increases, the tracking ability of our channel estimation scheme tends to be lost. As E_b/N_0 becomes smaller, the decision feedback error becomes more significant. As a

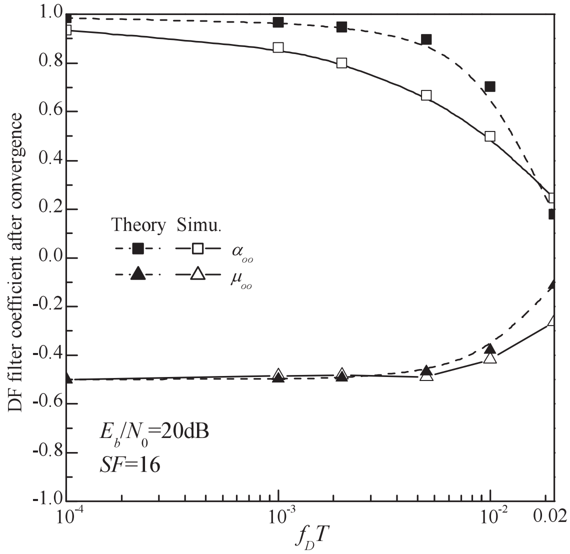

Fig. 4 Impact of Doppler spread.

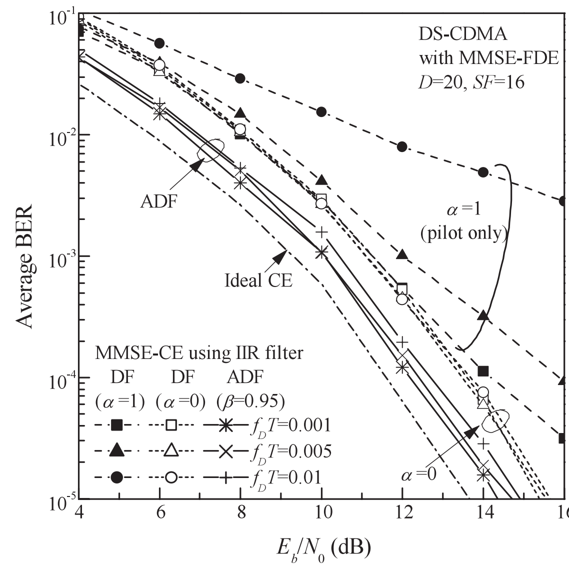

(a) SF=16.

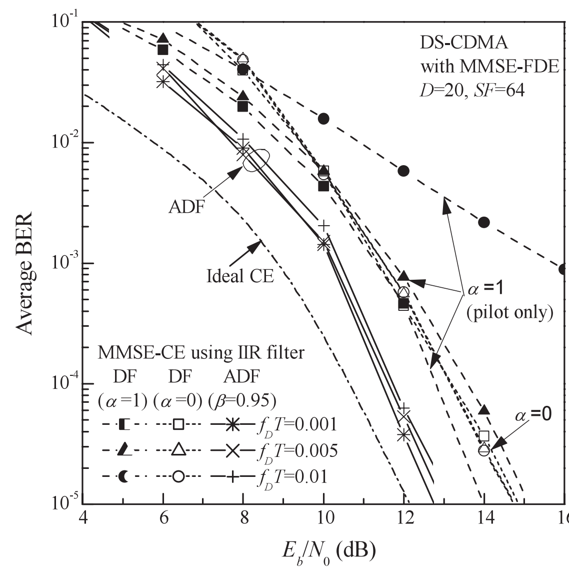

(b) SF=64.

Fig. 5 Performance comparison between DF-MMSE-CE and ADF-MMSE-CE.

consequence, the theoretical results tend to deviate from the simulated as f_DT increases and/or E_b/N_0 increases.

4.2 BER Performance

Figure 5 plots the simulated BER performance of DS-CDMA using ADF-MMSE-CE with the IIR filter for SF=16 and 64 as a function of E_b/N_0. Here, the frame length D is equal to 20 and f_DT varies from 0.001 to 0.01. In practical situation, the value of f_DT changes according to the change of the user's moving speed. The adaptive IIR filter can adapt the value of α to the optimum value so that the BER performance can always be minimized. It can be seen that ADF-MMSE-CE provides a fairly good BER performance for all f_DT values. For comparison, the BER performance of non-adaptive DF-MMSE-CE (α=0 and 1) is also plotted. When α=1 is used, the BER performance degrades significantly for large Doppler spread (i.e., f_DT=0.01). On the other hand, when α=0 is used, $\tilde{H}_{m-1}(k)$ is always used (see Eq. (10)) and a good tracking ability can be achieved but noise reduction is not sufficient. Therefore, the achievable BER performance is worse than ADF-MMSE-CE (β=0.95). ADF-MMSE-CE gives the best performance and is almost insensitive to f_DT. The E_b/N_0 degradation for BER=10^{-5} from the ideal CE is less than 1 dB. Part of this E_b/N_0 degradation is due to the pilot insertion loss of $10\log(20/19)$ = 0.23 dB.

Figure 6 shows the performance comparison of ADF-MMSE-CE using the IIR filter and the FLP filter. In the case of SF=16, Fig. 6(a) shows that the BER of the FLP filter is worse than that of the IIR filter for a low E_b/N_0 region. In the case of SF=64, the adaptive FLP filter cannot work well, since the symbol energy is distributed over SF chips and the low chip energy-to-noise power ratio E_c/N_0 produces large estimation error. No matter the value of μ, the FLP filter only uses the past two blocks to predict the current channel gain and has higher tracking ability; while the IIR filter uses about $1/(1-\alpha)$ past blocks and reduces the AWGN noise greatly. This results in the worse BER of the FLP filter than the IIR filter.

4.3 Impact of Frame Length

Phase correction using periodically inserted pilot chip blocks is used to avoid the error propagation beyond the frame. The E_b/N_0 loss due to the pilot insertion, given by $10\log D/(D-1)$ dB, can be reduced by increasing the frame length D. However, the tracking ability against fading may be lost. Figure 7 shows the impact of the frame length on the BER as a function of f_DT. We set E_b/N_0=14 dB for both SF=16 and 64 and the BERs of ADF-MMSE-CE with IIR

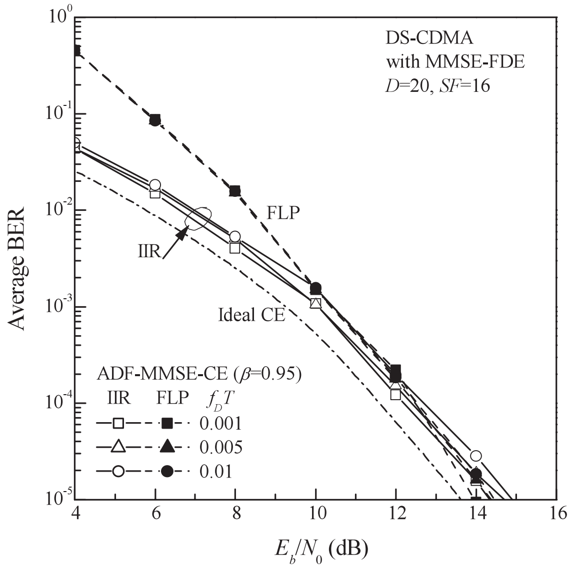

(a) SF=16.

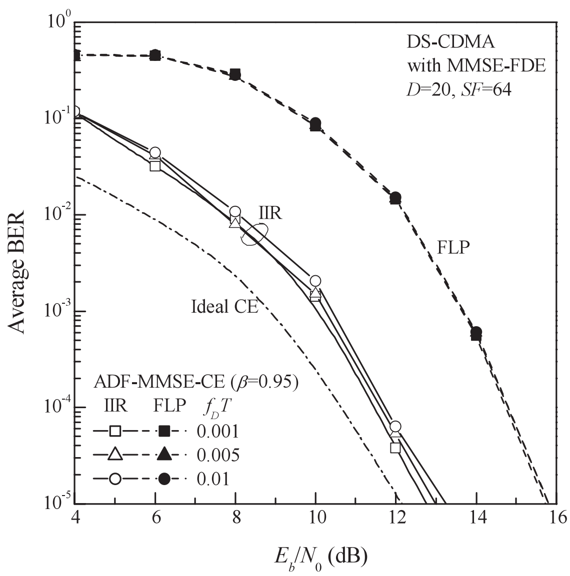

(b) SF=64.

Fig. 6 Performance comparison between adaptive IIR filter and adaptive FLP filter.

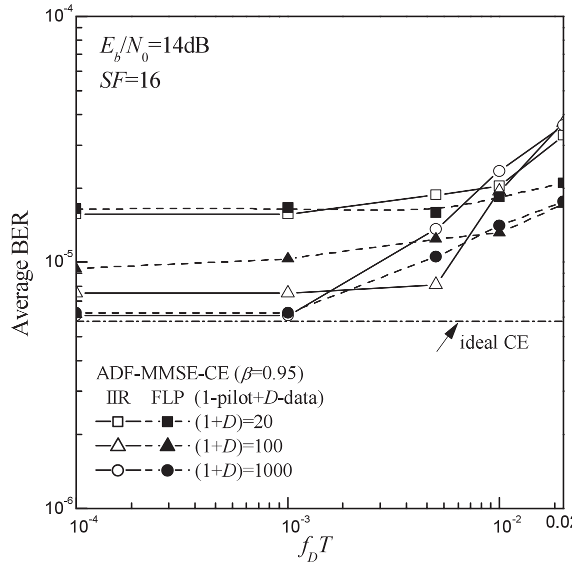

(a) SF=16.

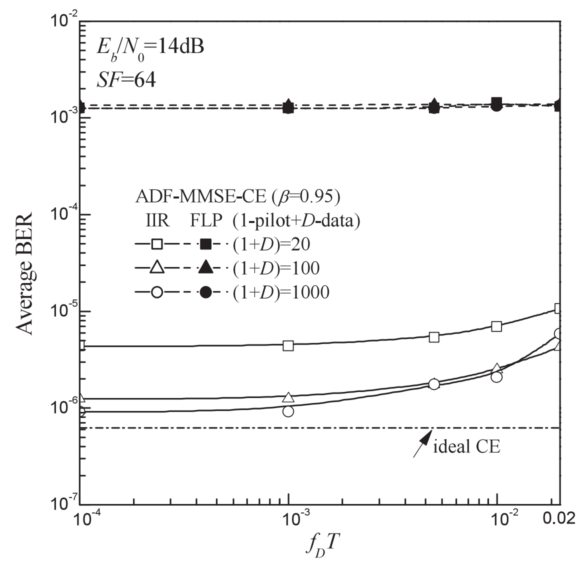

(b) SF=64.

Fig. 7 Impact of fame length D.

and FLP filters are plotted as a function of f_DT in Figs. 7(a) and (b). By increasing the value of D from 20 to 100, the pilot insertion loss decreases from 0.23 dB to 0.04 dB and the BER performance is slightly improved. Although the periodic phase correction is used, the decision feedback error will propagate within a frame for large Doppler spread and degrade the BER performance. Therefore, the frame length cannot be too large, e.g., D=1000. For high E_b/N_0, the Doppler spread is the predominant cause of decision error. The FLP filter has better tracking ability than the IIR filter. It can achieve a slightly smaller BER when $f_DT > 0.005$ in the case of SF=16. However, in the case of SF=64, since the chip energy-to-noise power ratio E_c/N_0 reduces and this produces large estimation error. The FLP filter uses only the past two blocks to predict the current channel gain; while the IIR filter uses more blocks, i.e., $1/(1-\alpha)$ past blocks. Therefore, the IIR filter can reduce more AWGN noise than the FIR filter. As shown in Fig. 7(b), that the performance of the IIR filter is much better than that of the FLP filter when SF=64.

5. Conclusions

In this paper, the adaptive decision feedback MMSE channel estimation (ADF-MMSE-CE) was proposed for DS-CDMA with MMSE-FDE. The adaptive infinite impulse response (IIR) filter and forward linear prediction (FLP) filter are utilized to track the changing channel conditions. The IIR filter coefficient α and the FLP filter coefficient μ are updated according to a recursive least-square (RLS) algorithm. In order to stop the error propagation beyond the frame due to the decision feedback, the channel estimate is phase corrected using periodically received pilot chip blocks. Computer simulation results have shown that the proposed ADF-MMSE-CE with IIR filter can achieve a very good tradeoff between the tracking ability against fading and noise reduction. Although the FLP filter is robust against fast fading, its BER performance is worse than IIR filter due to the low chip energy-to-noise power ratio when *SF* is large. In addition, this ADF-MMSE-CE, not limited to DS-CDMA, can be applied to multicarrier (MC-)CDMA with FDE in a fast fading channel.

References

[1] S. Sampei and T. Sunaga, "Rayleigh fading compensation for QAM in land mobile radio communications," IEEE Trans. Veh. Technol., vol.42, no.2, pp.137–147, May 1993.
[2] F. Ling, "Coherent detection with reference-symbol based estimation for direct sequence CDMA uplink communications," Proc. IEEE VTC'93-Spring, pp.400–403, May 1993.
[3] H. Andoh, M. Sawahashi, and F. Adachi, "Channel estimation filter using time-multiplexed pilot channel for coherent rake combing in DS-CDMA mobile radio," IEICE Trans. Commun., vol.E81-B, no.7, pp.1517–1526, July 1998.
[4] M.-A.R. Baissas and A.M. Sayeed, "Pilot-based estimation of time-varying multipath channels for coherent CDMA receivers," IEEE Trans. Signal Process., vol.50, no.8, pp.2037–2049, Aug. 2002.
[5] S. Coler, M. Ergen, A. Puri, and A. Bahai, "Channel estimation techniques based on pilot arrangement in OFDM systems," IEEE Trans. Broadcast., vol.48, no.3, pp.223–229, Sept. 2002.
[6] L. Mailaender, "Adaptive frequency-domain chip equalization for the MIMO CDMA downlink," Proc. IEEE VTC'04-Fall, pp.1766–1770, Los Angelos, U.S.A., Sept. 2004.
[7] J.Z. Wang and J. Chen, "Performance of wideband CDMA systems with complex spreading and imperfect channel estimation," IEEE J. Sel. Areas Commun., vol.19, no.1, pp.152–163, Jan. 2001.
[8] J.K. Cavers, "An analysis of pilot symbol assisted modulation for Rayleigh fading channels," IEEE Trans. Veh. Technol., vol.40, no.4, pp.686–693, Nov. 1991.
[9] W.G. Song and J.T. Lim, "Pilot-symbol aided channel estimation for OFDM with fast fading channels," IEEE Trans. Broadcast., vol.49, no.4, pp.398–402, Dec. 2003.
[10] C.H. Zhou, L. Meng, L. Gang, J. Wang, and W.D. Li, "An order-adaptive filter for channel estimation in DS-CDMA mobile systems," Proc. IEEE WCC-ICCT 2000, vol.1, pp.355–358, Aug. 2000.
[11] K. Takeda and F. Adachi, "Pilot-assisted channel estimation based on MMSE criterion for DS-CDMA with frequency-domain equlization," Proc. IEEE VTC'05-Spring, pp.447–451, Stockholm, Sweden, May 2005.
[12] F. Adachi, "Adaptive differential detection using linear prediction for M-ary DPSK," IEEE Trans. Veh. Technol., vol.47, no.3, pp.909–918, Aug. 1998.
[13] D. Falconer, S.L. Ariyavisitakul, A. Benyamin-Seeyar, and B. Eidson, "Frequency domain equalization for single-carrier broadband wireless systems," IEEE Commun. Mag., vol.40, no.4, pp.58–66, April 2002.
[14] J.-J. van de Beek, O. Edfors, M. Sandell, S.K. Wilson, and P.O. Borjesson, "On channel estimation in OFDM systems," Proc. IEEE VTC'95, pp.815–819, Chicago, Illisnois, USA, July 1995.
[15] T. Fukuhara, H. Yuan, Y. Takeuchi, and H. Kobayashi, "A novel channel estimation method for OFDM transmission technique under fast time-variant fading channel," Proc. IEEE VTC'03-Spring, pp.2343–2347, Jeju, Korea, April 2003.
[16] S. Haykin, Adaptive filter theory, Prentice-Hall, Englewood Cliffs, NJ, 1991.
[17] B. Widrow and S. Stearns, Adaptive signal processing, Prentice-Hall, Englewood Cliffs, NJ, 1985.
[18] W.C. Jakes, Jr., ed., Microwave mobile communications, Wiley, New York, 1974.
[19] K. Takeda, T. Itagaki, and F. Adachi, "Joint use of frequency-domain equalization and transmit/receive antenna diversity for single-carrier transmissions," IEICE Trans. Commun., vol.E87-B, no.7, pp.1946–1953, July 2004.

Appendix: Convergence Performance Analysis of Filter Coefficients

(1) IIR filter

Equation (13) can be written as

$$\begin{cases} \Theta_m(k) = \displaystyle\sum_{l=0}^{m} \beta^l \mathrm{Re}\left\{A_{m-l}(k)B^*_{m-l}(k)\right\} \\ \Omega_m(k) = \displaystyle\sum_{l=0}^{m} \beta^l \left|B_{m-l}(k)\right|^2 \end{cases} \tag{A·1}$$

for $k = 0 \sim N_c - 1$. Assuming the received signal sequence is a stationary process and $\beta < 1$, the ensemble average values of Θ_m and Ω_m may approach [12]:

$$\begin{cases} E[\Theta_m(k)] \approx (1-\beta)^{-1} E[\mathrm{Re}\{A_m(k)B^*_m(k)\}] \\ E[\Omega_m(k)] \approx (1-\beta)^{-1} E[|B_m(k)|^2] \end{cases}. \tag{A·2}$$

Using Eq. (14), $A_m(k)$ and $B_m(k)$ are given by

$$\begin{cases} A_m(k) = R_m(k) - \tilde{H}_{m-1}(k)\tilde{S}_m(k) \\ B_m(k) = \tilde{S}_m(k)\left\{\tilde{H}_{m-1}(k) - \bar{H}^{IIR}_{m-2}(k)\right\} \end{cases}. \tag{A·3}$$

As mentioned in Sect. 2.3, the noise in the channel estimate $\tilde{H}_m(k)$ is greatly reduced by using the delay-time domain windowing technique. If we approximate the residual channel estimation error in $\tilde{H}_m(k)$ as a new zero-mean Gaussian noise $\tilde{\Pi}_m(k)$, the mth block channel estimate $\tilde{H}_m(k)$ can be expressed as

$$\tilde{H}_m(k) = \sqrt{2E_c/T_c} H_m(k) + \tilde{\Pi}_m(k), \tag{A·4}$$

where

$$E[\left|\tilde{\Pi}_m(k)\right|^2] = (N_g/N_c) \cdot (2N_0/T_c). \tag{A·5}$$

Substitute α in Eq. (10) with α_m, we have the IIR filter output expressed as

$$\bar{H}^{IIR}_m(k) = \sum_{l=1}^{m} \tilde{H}_l(k)(1-\alpha_l) \prod_{j=l+1}^{m} \alpha_j + \tilde{H}_0(k) \prod_{j=1}^{m} \alpha_j. \tag{A·6}$$

In order to simplify the analysis, we neglect the effects of the AWGN and decision feedback error. Therefore, we use $\bar{H}^{IIR}_m(k) \approx \sqrt{2E_c/T_c} H_m(k)$ and $\tilde{S}_m(k) \approx S_m(k)$ and $A_m(k)$ and $B_m(k)$ can be approximated as

$$\begin{cases} A_m(k) \approx \sqrt{2E_c/T_c} S_m(k)\{H_m(k) - H_{m-1}(k)\} \\ \qquad\qquad + \Pi_m(k) - S_m(k)\tilde{\Pi}_{m-1}(k) \\ B_m(k) \approx \sqrt{2E_c/T_c} S_m(k)\{H_{m-1}(k) - H_{m-2}(k)\} \\ \qquad\qquad + S_m(k)\tilde{\Pi}_{m-1}(k) \end{cases}. \tag{A·7}$$

On the other hand, assuming that path gains $\{h_{m,l};\ l = 0 \sim L-1\}$ are independent with $\sum_{l=0}^{L-1} E[|h_{m,l}|^2] = 1$ and they have the identical autocorrelation function $\rho(n)$ as [18]

$$\rho(n) = E[h_{m,l}h^*_{m-n,l}] \Big/ \sqrt{E[|h_{m,l}|^2]E[|h_{m-n,l}|^2]}. \qquad \text{(A· 8)}$$

The time autocorrelation function $R(n;k)$ of the kth frequency channel gain $H_m(k)$ is equal to $\rho(n)$ as

$$R(n;k) = E[H_m(k)H^*_{m-n}(k)] = \rho(n). \qquad \text{(A· 9)}$$

Substituting Eq. (A· 7) into Eq. (A· 2) and using Eq. (A· 8), we obtain

$$\begin{cases} E[\Theta_m(k)] = -\dfrac{2N_0/T_c}{(1-\beta)}\left[\dfrac{E_c}{N_0}(1+\rho(2)-2\rho(1)) + \dfrac{N_g}{N_c}\right] \\ E[\Omega_m(k)] = \dfrac{4N_0/T_c}{(1-\beta)}\left[\dfrac{E_c}{N_0}(1-\rho(1)) + \dfrac{N_g}{2N_c}\right] \end{cases}. \qquad \text{(A· 10)}$$

Therefore, substituting Eq. (A· 10) into Eq. (12), we obtain Eq. (20).
(2) FLP filter
In the similar way as the IIR filter, we can derive the convergence value for FLP filter as

$$\begin{cases} E[\Theta'_m(k)] = E[\Theta_m(k)] \\ E[\Omega'_m(k)] = \dfrac{4N_0/T_c}{(1-\beta)}\left[\dfrac{E_c}{N_0}(1-\rho(1)) + \dfrac{N_g}{N_c}\right] \end{cases}. \qquad \text{(A· 11)}$$

Substituting Eq. (A· 11) into Eq. (17), we obtain Eq. (21).

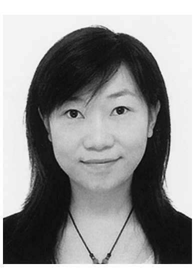

Le Liu received B.S. and M.S. degrees in electrical engineering from Beijing University of Posts and Telecommunications (BUPT), Beijing, China, in 2000 and 2003, respectively. From April 2003 to September 2004, she took part in the collaboration between the National Institute of Information and Communications Technology (NICT), Japan, and BUPT on the 4G Wireless Telecommunications Project. Currently, she is a Ph.D. candidate at the Dept. of Electrical and Communication Engineering, Graduate School of Engineering, Tohoku University with a scholarship from the Japanese government. Her research interests include digital signal transmission techniques for direct sequence CDMA and multicarrier CDMA.

Fumiyuki Adachi received the B.S. and Dr. Eng. degrees in electrical engineering from Tohoku University, Sendai, Japan, in 1973 and 1984, respectively. In April 1973, he joined the Electrical Communications Laboratories of Nippon Telegraph & Telephone Corporation (now NTT) and conducted various types of research related to digital cellular mobile communications. From July 1992 to December 1999, he was with NTT Mobile Communications Network, Inc. (now NTT DoCoMo, Inc.), where he led a research group on wideband/broadband CDMA wireless access for IMT-2000 and beyond. Since January 2000, he has been with Tohoku University, Sendai, Japan, where he is a Professor of Electrical and Communication Engineering at the Graduate School of Engineering. His research interests are in CDMA wireless access techniques, equalization, transmit/receive antenna diversity, MIMO, adaptive transmission, and channel coding, with particular application to broadband wireless communications systems. From October 1984 to September 1985, he was a United Kingdom SERC Visiting Research Fellow in the Department of Electrical Engineering and Electronics at Liverpool University. Dr. Adachi served as a Guest Editor of IEEE JSAC for special issue on Broadband Wireless Techniques, October 1999 and for special issue on Wideband CDMA I, August 2000, and Wideband CDMA II, Jan. 2001. He is an IEEE Fellow and was a co-recipient of the IEEE Vehicular Technology Transactions Best Paper of the Year Award 1980 and again 1990 and also a recipient of Avant Garde award 2000. He was a recipient of IEICE Achievement Award 2002 and a co-recipient of the IEICE Transactions Best Paper of the Year Award 1996 and again 1998. He was a recipient of Thomson Scientific Research Front Award 2004.